

# Constraining the astrophysical S factor of the $^3\text{He}(\alpha, \gamma)^7\text{Be}$ reaction

M. CARMONA-GALLARDO<sup>1</sup>, A. ROJAS<sup>2</sup>, B.S. NARA SINGH<sup>3</sup>, C. AKERS<sup>2,3</sup>, O. AVIV<sup>4</sup>,  
M.J.G. BORGE<sup>1</sup>, G. CHRISTIAN<sup>2</sup>, B. DAVIDS<sup>2</sup>, J. FALLIS<sup>2</sup>, B. R. FULTON<sup>3</sup>, U. HAGER<sup>5</sup>,  
G. HAQUIN<sup>4</sup>, M. HASS<sup>6</sup>, D. A. HUTCHEON<sup>2</sup>, Y. NIR-EL<sup>4</sup>, D. OTTEWELL<sup>2</sup>, C. RUIZ<sup>2</sup>,  
S.K.L. SJUE<sup>2</sup>, O. TENGBLAD<sup>1</sup>, R. YANIV<sup>4</sup> and Z. YUNGREIS<sup>4</sup>

<sup>1</sup>*Instituto de Estructura de la Materia-CSIC, Serrano 113-Bis, 28006E-Madrid, Spain*

<sup>2</sup>*TRIUMF, V6T 2A3, Vancouver, BC, Canada*

<sup>3</sup>*University of York, YO10, York, UK*

<sup>4</sup>*Soreq Research Centre, Yavne, Israel*

<sup>5</sup>*Colorado School of Mines, Golden, Colorado, USA*

<sup>6</sup>*Weizmann Institute, Rehovot 76100, Israel*

*E-mail: m.carmona.gallardo@gmail.com*

(Received September 10, 2014)

The cross section of the  $^3\text{He}(\alpha, \gamma)^7\text{Be}$  reaction has been widely studied both from the theoretical and the experimental fronts due to its relevance to the standard solar model and to the Big Bang Nucleosynthesis calculations. We report here on cross section measurements in the energy region  $E_{\text{c.m.}}=1\text{-}3$  MeV using the direct recoil counting method in an attempt to resolve the discrepancies among the previous data sets and calculations in this energy region and thus to constrain the extrapolations of the  $S_{34}(E)$  curve to astrophysical energies.

**KEYWORDS:** Nuclear Reaction, Astrophysical S factor, DRAGON separator,  $^3\text{He}(\alpha, \gamma)^7\text{Be}$

## 1. Introduction

The astrophysical S factor of the  $^3\text{He}(\alpha, \gamma)^7\text{Be}$  reaction is one of the nuclear input-parameters to the Standard Solar Model (SSM) [1]. In particular, this reaction rate is influential in the predictions of the solar neutrino fluxes from the  $^8\text{B}$  and  $^7\text{Be}$  decays in the proton-proton chain [2]. The importance of this reaction is highlighted when one considers the SSM parameters. Particularly, the uncertainty in the astrophysical S factor is the third largest error contribution (5.2%) ranking after the diffusion parameter (15%) and the astrophysical S factor of the  $^7\text{Be}(p, \gamma)^8\text{B}$  reaction (7.7%) [3].

Moreover, the  $^3\text{He}(\alpha, \gamma)^7\text{Be}$  reaction is part of the main reaction network involved in the Big Bang nucleosynthesis. Therefore, precise determination of the reaction rate is also crucial in the so called  *$^7\text{Li}$  problem*, i.e. the discrepancy between the inferred primordial  $^7\text{Li}$  abundance from direct astrophysical observations and that obtained using the Big Bang nucleosynthesis calculations [4].

The initial approaches described the  $^3\text{He}(\alpha, \gamma)^7\text{Be}$  reaction as a direct extra-nuclear capture process, where an electromagnetic transition connects the initial scattering state and the final bound states in the  $^7\text{Be}$  nucleus [5, 6]. Considering the fact that at the low astrophysical energies the  $\ell=0$  orbital angular momentum dominates, an E1 transition connects the  $^3\text{He}+^4\text{He}$  initial scattering state having the total angular momentum  $J_i=1/2^+$  to the ground,  $J_f=3/2^-$ , or first excited,  $J_f=1/2^-$ , states in the final  $^7\text{Be}$  system (see Fig. 1). As the energy of the reaction is increased higher partial wave contributions, mainly  $\ell=2$ , yet dominantly of E1 type, would become more important [7]. Extensive potential and microscopic model calculations, e.g. see Refs. [7, 8], followed the first studies using diverse approaches, such as different potentials, in order to obtain the scattering and bound wave

functions and thereby to reproduce the energy dependence of the cross section. Ab initio calculations using microscopic molecular dynamics constitute the most recent and advanced approach that has been employed to study this reaction [9].

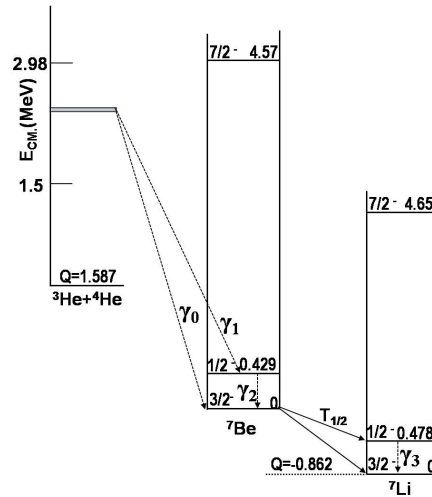


**Fig. 1.** Decay scheme of the  ${}^3\text{He}+{}^4\text{He}$  direct capture reaction and the subsequent decay of  ${}^7\text{Be}$  to  ${}^7\text{Li}$ . The energies are displayed in MeV and the spin and parities of the states are indicated. The capture reaction Q-value is 1.587 MeV. The energy of the electromagnetic radiations  $\gamma_0$  and  $\gamma_1$ , so-called prompt  $\gamma$ -rays, depend on the reaction energy. The first excited state and the ground state in  ${}^7\text{Be}$  are connected by  $\gamma_2$ . The  ${}^7\text{Be}$  nucleus in the ground  $3/2^-$  state is unstable and decays via electron capture to  ${}^7\text{Li}$  with  $T_{1/2}=53.24(4)$  days and with a branching ratio of 10.44(4)% to the first excited state at 478 keV in  ${}^7\text{Li}$ , which subsequently de-excites by emitting the corresponding  $\gamma_3$ -ray.

Since the cross section of the  ${}^3\text{He}(\alpha,\gamma){}^7\text{Be}$  reaction decreases with decreasing energy, it is experimentally impossible to measure the cross section at the low astrophysical energies of interest (e.g. the Gamow Energy in the Sun is at  $\sim 22$  keV). Therefore, theoretical models are used to extrapolate the astrophysical S factor data obtained at higher energies towards zero energy ( $S_{34}(0)$ ).

The cross section of this reaction has been measured in a wide range of 93-3130 keV centre of mass energies using different techniques. Large discrepancies are observed in the region 1000-3000 keV, where only data from Parker *et al.* [10] and the ERNA collaboration [11] were available before the measurements performed by our collaboration. Also, discrepancies are seen in the same energy region when comparing different calculations, e.g. Ref. [8, 9, 12–14], not only in the absolute scale of the cross section, but also in its dependence with energy. Recently, as a part of our strategy to study this reaction, we measured the cross section of the  ${}^3\text{He}(\alpha,\gamma){}^7\text{Be}$  reaction in the region  $E_{\text{c.m.}} \sim 700\text{--}2800$  keV by using the activation method. Three data points obtained with low statistical error contribution [15] particularly show a good agreement with the ERNA data [11] and disagree with those from Parker *et al.* [10]. A good agreement of our results and those from the ERNA collaboration is also seen when comparing with the recent measurements obtained by the ATOMKI collaboration using the activation technique [16]. Nevertheless, independent measurements in the same energy region using complementary techniques and setups are required in order to improve the reliability of the energy dependence of the S factor in this energy range and thus refine theoretical model extrapolations to zero energy. Moreover, measurements in this region constrain the influence of short range nuclear interactions on the cross section needed because the reaction may not be purely external [9]. In this work, our strategy consisted of using the direct recoil counting method in the same energy range of  $E_{\text{c.m.}}=1000\text{--}3000$  keV in order to complement our activation technique work [15].

## 2. Direct Recoil Counting Technique

In the direct recoil counting method, the  $^7\text{Be}$  nuclei produced at forward angles in the radiative capture reaction are counted directly. In order to do so, the recoils must be separated from the copious amount of unreacted beam particles before being counted in a detector. For this purpose the **D**etector of **R**ecoils **A**nd **G**ammas **O**f Nuclear **R**eactions (DRAGON) separator was used [17].  $^4\text{He}$  beams at four different energies impinged onto a  $^3\text{He}$  gas target and the  $^7\text{Be}$  recoils were counted in a double sided silicon strip detector (DSSSD) placed at the focal plane of the separator. Typically, the gas target had pressures of 6 Torr and its areal density,  $N_{^3\text{He}}^T$ , was determined by considering an ideal gas behaviour. The total number of beam particles,  $N_{^4\text{He}}^B$ , was estimated from hourly Faraday cup readings and normalised using the scattered particle spectra taken with two silicon detectors placed at  $30^\circ$  and  $57^\circ$  with respect to beam direction. Three important features must be taken into account here in order to determine the absolute cross section [18], namely: (I) in order to maximise the recoil transmission through the gas target a windowless gas target was used *whose profile needs to be characterised*, (II) the  $^7\text{Be}$  recoils are separated from the unreacted beam particles by kinetic energy and charge state selections, *therefore the charge state distribution of the recoils entering DRAGON needs to be determined*, and (III) as this is the most symmetric reaction studied using DRAGON and the recoil cone angle is slightly larger than the geometrical acceptance of the separator, *the transmission of the recoils through the separator and the sensitivity to various parameters of the separator must be estimated*. In addition, good beam suppression capability of the separator is essential.

### 2.1 Target Density Profile

The  $^3\text{He}$  gas pressure was maintained inside a 11 cm windowless target cell using a differential pumping system. Therefore, there could be some residual gas in the downstream and upstream pumping tubes which will influence the recoil transmission as the reaction can take place far from the centre of the cell. Thus, the target density profile was determined experimentally by using the  $^3\text{He}(^{12}\text{C}, ^{14}\text{N}\gamma)p$  reaction. The  $^{12}\text{C}$  beam energy was set to populate the broad 14.46 MeV state in the  $^{15}\text{O}$  nucleus which decays by proton emission populating the 6.44 MeV state in  $^{14}\text{N}$ ; this subsequently de-excites via the emission of the corresponding  $\gamma$ -ray. The relative yield of the 6.44 MeV  $\gamma$ -ray at different positions with respect to the centre of the target cell and parallel to the beam axis was measured using a shielded BGO detector. The yield was normalised considering the target pressure and the scattered beam particles detected in the silicon detector placed at  $30^\circ$ . A correction of the yield due to the differences in probability for the reaction to take place at different target positions (or different beam energies due to the  $^{12}\text{C}$  energy loss in the  $^3\text{He}$  target) was considered by taking the Breit-Wigner description of the resonance state into account. The resulting experimental target density profile is shown in Fig. 2.

### 2.2 Charge State Distribution

The DRAGON separator was tuned to select the  $3^+$  charge state ( $^7\text{Be}^{3+}$ ) for the two highest beam energies studied and the  $2^+$  charge state ( $^7\text{Be}^{2+}$ ) for the two lowest ones. Thus, it was needed to determine the fraction of the recoils entering the separator for the different charge states. Based on the fact that the charge state distribution of ions crossing a material is independent of both the initial charge state and the incoming isotope, but rather depends on the ion velocity and target atomic number, we used a  $^9\text{Be}$  beam and a  $^3\text{He}$  gas target to determine the charge state distribution. The  $^9\text{Be}$  velocities were matched to those corresponding to the  $^7\text{Be}$  recoils created at the centre of the target cell following the capture reaction. The charge state fractions for  $^9\text{Be}$  ions after passing through the target were measured by selecting the corresponding rigidity in the first magnetic dipole and measuring the current in the Faraday cup placed after it. The measurements were performed using  $\sim 1$  Torr and  $\sim 6$  Torr  $^3\text{He}$  gas pressures, showing that the equilibration of the charge state is reached

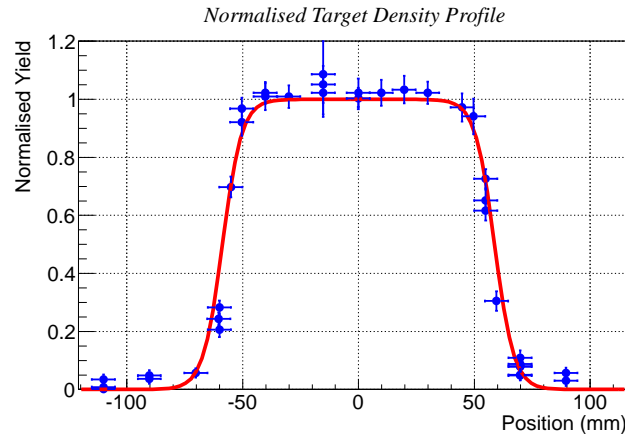


**Fig. 2.** Experimental target density profile along the beam direction. The blue dots show the 6.44 MeV  $\gamma$  yield at different positions relative to the value at centre of the target cell (0 mm). The red curve fits the experimental points using the function  $\frac{1}{1+e^{(|z|-R)/a}}$  where  $R$  and  $a$  are free parameters.

within these pressures and thus the recoil charge state distribution is the same independently of where the recoils are created across the length of the target [19].

### 2.3 Recoil Transmission

The transmission of the recoils through DRAGON was estimated by performing Monte Carlo simulations with the GEANT 3 DRAGON code, which was adapted to recreate the experimental conditions of our measurements. Input parameters such as beam energies, emittance (estimated according to ISAC-I specifications and experimental beam transmissions) and the measured target density profile shown in Fig. 2 were considered. Based on the fact that no resonances are expected in this energy region, the  ${}^3\text{He}(\alpha, \gamma){}^7\text{Be}$  capture reaction probability was assumed to be constant across the target length. Therefore, the simulated  ${}^7\text{Be}$  recoil distribution along the beam direction follows the target density profile function. Isotropic angular distributions for the prompt  $\gamma_0$  and  $\gamma_1$  rays emitted with branching ratios extrapolated from the values given in Ref. [14] were also included. The settings of the different electromagnetic elements of the simulated separator were taken from the measured values using NMR-probes. The resulting recoil transmissions are between  $(51.3 \pm 0.3^{+3.0}_{-3.8})\%$  and  $(71.7 \pm 0.6^{+3.0}_{-6.7})\%$ , where the statistical and systematic uncertainty contributions are given separately. The systematic errors were obtained by studying the sensitivity of the transmission to different inputs, such as the target density profile function and the prompt  $\gamma$ -ray angular distributions. For the four energies, a beam displacement of  $\pm 1$  mm in the transverse directions to the beam axis gives the dominant contribution to the systematic error. The spread in the recoil energy is the most influential parameter on the transmission.

## 3. Analysis and Results

The reaction was studied using  ${}^4\text{He}^{2+}$  beam energies of 3.52, 4.72, 5.17 and 6.55 MeV. The beam suppression studies performed by tuning the separator to select the  ${}^7\text{Be}^{3+}$  recoils for the highest beam energy showed a high suppression of  $> 1.2 \cdot 10^{14}$  in terms of incoming beam particles divided by transmitted beam particles through the separator [20]. However, for the  ${}^7\text{Be}^{2+}$  selection, the contribution of the unreacted scattered beam is expected to be higher in the recoil peak due to the available  $2^+$  charge state of the beam. In order to study the background contribution from the beam when DRAGON was tuned to the  $2^+$  charge state, a Micro-Channel Plate (MCP) device was placed upstream of the

DSSSD. The time of flight of the ions between the two plates of the MCP was measured together with the energy in the DSSSD. Fig. 3 shows in the upper panel the time of flight from the MCP measurements versus the energy of the ions detected in the DSSSD. As can be observed the  $^7\text{Be}$  are nicely separated from the unreacted beam particles. Thus, the recoil peak, seen in the lower panel of Fig. 3, can be integrated without being influenced by the beam particles.

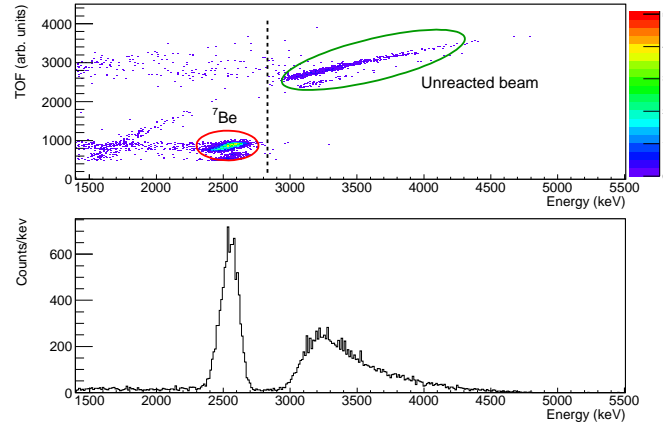


**Fig. 3.** The upper panel shows the two-dimensional histogram of the time of flight obtained from the MCP versus the energy of the events detected in the DSSSD, for a beam energy of 4716 keV. The black dashed line separates the  $^7\text{Be}$  recoils from the unreacted beam particles. The lower panel shows the one-dimensional histogram projected onto the energy axis of the two-dimensional histogram. The most intense peak around 2500 keV shows the  $^7\text{Be}$  recoils, which is separated from any unreacted beam particles.

The total yield of the recoils,  $Y_{^7\text{Be}}$ , was then estimated from the integrated counts in the recoil peak,  $Y_{\text{DSSSD}}$ , (cf. Fig. 3) by using the expression:

$$Y_{^7\text{Be}} = \frac{Y_{\text{DSSSD}}}{t_{\ell} \cdot q_f \cdot \epsilon_{\text{DRAGON}} \cdot \epsilon_{\text{DSSSD}}} \quad (1)$$

where  $t_{\ell}$  is the livetime of the acquisition system,  $q_f$  is the given  $^7\text{Be}$  charge state fraction,  $\epsilon_{\text{DRAGON}}$  is the recoil transmission obtained from the GEANT 3 simulations, and  $\epsilon_{\text{DSSSD}}$  is the DSSSD efficiency. The astrophysical S factor is then calculated from the cross section,  $\sigma_{34} = Y_{^7\text{Be}} / (N_{^3\text{He}}^T \cdot N_{^4\text{He}}^B)$ , as:  $S_{34} = \sigma_{34} \cdot E_{\text{c.m.}} \cdot e^{2\pi\eta}$  where  $\eta$  is the Sommerfeld parameter and the centre of mass energy,  $E_{\text{c.m.}}$ , is calculated assuming that the reaction takes place at the centre of the target cell.

Complementing our recoil detection measurements, a measurement using the activation technique was also carried out at TRIUMF. Following the same procedure used for our activation measurements in Madrid [15], we collected the  $^7\text{Be}$  recoils in a copper catcher placed at 85 cm downstream the centre of the target cell. The subsequent delayed  $\gamma$ -ray activity from the de-excitation of the  $^7\text{Li}$  in the catcher was measured using a low background HPGe detector station.

The **preliminary** results for the astrophysical S factor are shown in Fig. 4 together with the Parker *et al.* data and those obtained after the measurements at Weizmann in 2004 [21]. A good agreement can be seen between the values obtained using the direct recoil counting technique at TRIUMF (black dots) and the measurements using the activation technique in Madrid (red dots). They both also agree with the ERNA and the ATOMKI data and clearly disagree with the results from Parker *et al.*. Among the different theoretical models, the ab-initio calculations by Thomas Neff [9], which quote a  $S_{34}(0)$  value of 0.593 keV·b can reproduce our Madrid and TRIUMF data from 0.7 to 3 MeV as well as those

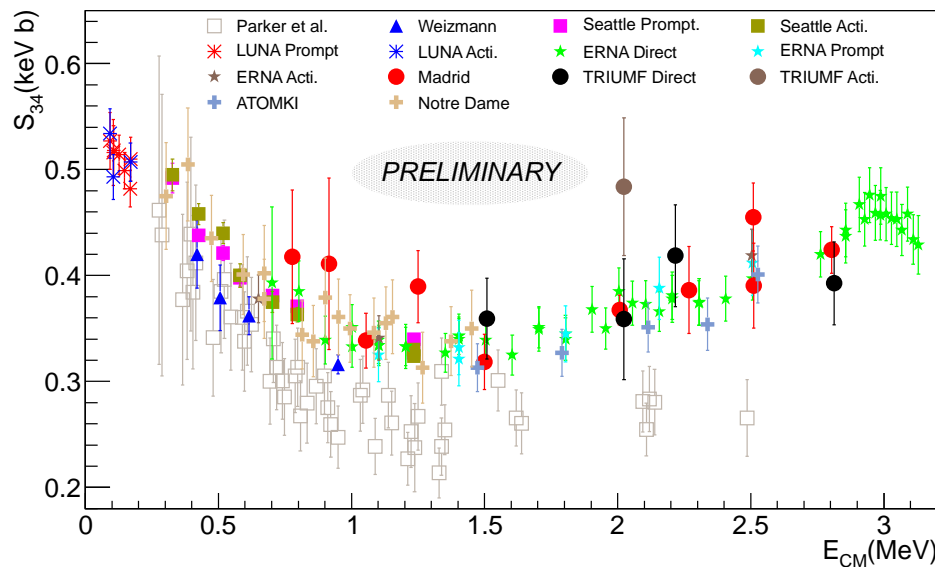


**Fig. 4.** The  $S$  factors obtained are shown for the Madrid experiment using the activation technique (red filled circles) [15] and for the TRIUMF data using the direct recoil counting method (black filled circles). The brown filled circle shows the value obtained using the activation technique at TRIUMF. The  $S$  factors from Parker *et al.* [10] and LUNA [22, 23], ERNA [11], ATOMKI [16], Weizmann [21], Notre Dame [24] and Seattle [25] collaborations are also shown for comparison.

from the LUNA collaboration that cover the lowest energy region, without using any normalisation factor.

## References

- [1] E. G. Adelberger *et al.*, Rev. Mod. Phys., **83** No. 1 (2011) 195
- [2] R. H. Cyburt and B. Davids, Phys. Rev. C, **78** (2008) 064614
- [3] W. C. Haxton, R. G. H. and A. M. Serenelli, Annu. Rev. Astro. Astrophys. **51** (2013) 21
- [4] R. H. Cyburt, B. D. Fields and K. A. Olive, J. Cosmol. Astropart. Phys. **11** (2008) 012
- [5] R. F. Christy and I. Duck, Nucl. Phys. **24** (1961) 89
- [6] T. A. Tombrello and P. D. Parker, Phys. Rev. **131** (1963) 2582
- [7] B. T. Kim, T. Izumoto and K. Nagatani, Phys. Rev. C **23** (1981) 33
- [8] T. Kajino, Nucl. Phys. A **460** (1986) 351
- [9] T. Neff, Phys. Rev. Lett. **106** (2011) 042502
- [10] P. D. Parker and R. W. Kavanagh, Phys. Rev. **131** (1963) 2578
- [11] A. Di Leva *et al.*, Phys. Rev. Lett. **102** (2009) 232502
- [12] K. M. Nollert, Phys. Rev. C. **63** (2001) 054002
- [13] P. Mohr, Phys. Rev. C **79** (2009) 065804
- [14] R. H. Cyburt and B. Davids, Phys. Rev. C. **78** (2008) 064614
- [15] M. Carmona-Gallardo *et al.*, Phys. Rev. C. **86** (2012) 032801(R)
- [16] C. Bordeanu *et al.*, Nucl. Phys. A **908** (2013) 1
- [17] D. A. Hutcheon *et al.*, Nucl. Instr. and Meth. A **498** (2003) 190
- [18] B. S. Nara Singh, Acta Phys. Pol., **44**, (2013) 511
- [19] M. Carmona-Gallardo *et al.*, Eur. Phys. J. Web of Conferences **66** (2014) 07003
- [20] S. K. L. Sjøe *et al.*, Nucl. Instr. and Meth. A **700** (2013) 179
- [21] B. S. Nara Singh *et al.*, Phys. Rev. Lett. **93** (2004) 262503
- [22] F. Confortola *et al.*, Phys. Rev. C **75** (2007) 065803
- [23] D. Bemmerer *et al.*, Phys. Rev. Lett. **97** (2006) 122502
- [24] A. Kontos *et al.*, Phys. Rev. C **87** (2013) 065804
- [25] T. A. D. Brown *et al.*, Phys. Rev. Lett. **76** (2007) 055801